A Long Crack Penetrating a Circular Inhomogeneity

The authors dedicate this paper to Professor Piero Villaggio on the occasion of his 70th birthday. Roberto Ballarini would like to express his deep respect for Professor Villaggio's contributions to science, and his sincere appreciation for the warmth and generosity Piero demonstrated towards him and his wife Susan during their visits to Pisa

YUPING WANG and ROBERTO BALLARINI*
Department of Civil Engineering, Case Western Reserve University, Bingham Building, 10900 Euclid Avenue, Cleveland, OH 44106-7201, USA

Abstract. This paper presents the effects of elastic mismatch and crack-tip position on the stress intensity factors of a long crack penetrating a circular inhomogeneity. The analysis relies on closed-form solutions, derived using complex variable techniques, for the stresses and displacements produced by dislocations positioned inside and outside the inhomogeneity. Dislocation distributions are introduced to express the traction boundary condition along the crack surfaces as a system of singular integral equations, whose solution is obtained through a numerical procedure. It is shown that if the elastic mismatch is interpreted correctly, then the stress intensity factors of this micromechanical model are very good approximations to those computed using a Monte Carlo finite element model of a long crack in a polycrystalline plate with compliant grain boundaries.

Key words: Crack, Transformation, Inhomogeneity, Stress intensity factor.

1. Introduction

To better understand the fracture behavior of polycrystalline plates, Abdel-Tawab and Rodin (1993), Ballarini *et al.* (1999) and Wang and Ballarini (2002) have developed finite element based micromechanical models for predicting the statistics of the microscopic (local) stress intensity factors and the energy release rate of a crack in a columnar aggregate of randomly oriented, perfectly bonded, orthotropic crystals (grains) under plane deformation. Figure 1 shows a typical model of a cracked crystalline plate analyzed by Wang and Ballarini (2002). An aggregate of isotropic grains with shear modulus μ_g, Poisson ratio ν_g, and average linear dimension d, perfectly bonded to each other through grain boundaries with shear modulus μ_{gb}, Poisson ratio ν_{gb}, and thickness t, is constructed m times using a Poisson–Voronoi tessellation procedure. In this stochastic model the expected number of grains within a unit area for each realization is defined by n, and the crack length is of constant length a. The loading consists of a prescribed displacement Δ along one edge of the plate.

Figure 2 shows the statistics of the local mode-I stress intensity factor, K_1^{loc}, calculated using the finite element method, for three values of n and for $m = 500$ Monte Carlo simulations. The microscopic stress intensity factor is normalized with respect to a reference value, K_1^{ref}, associated with a homogeneous cracked plate whose elastic moduli $\bar{\mu}$ and $\bar{\nu}$ correspond

---

*Author for correspondence. e-mail: rxb@po.cwru.edu
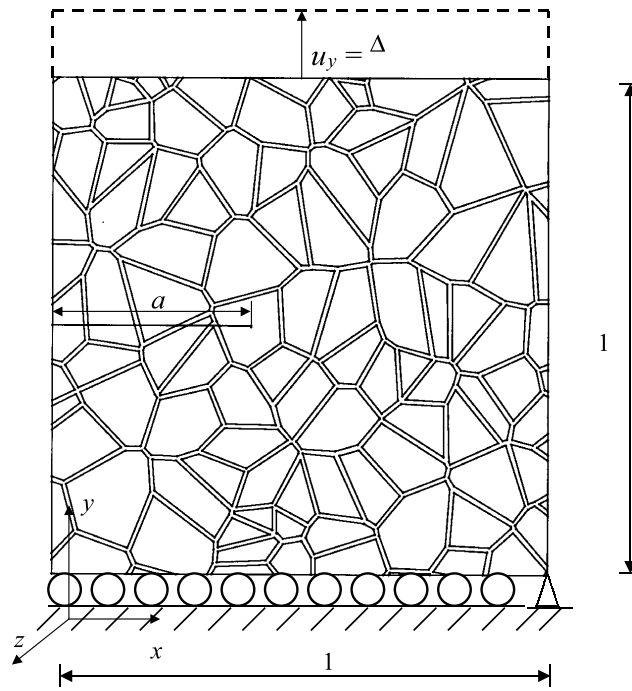
Figure 1. Micromechanical model of a cracked polycrystalline plate with compliant grain boundaries.
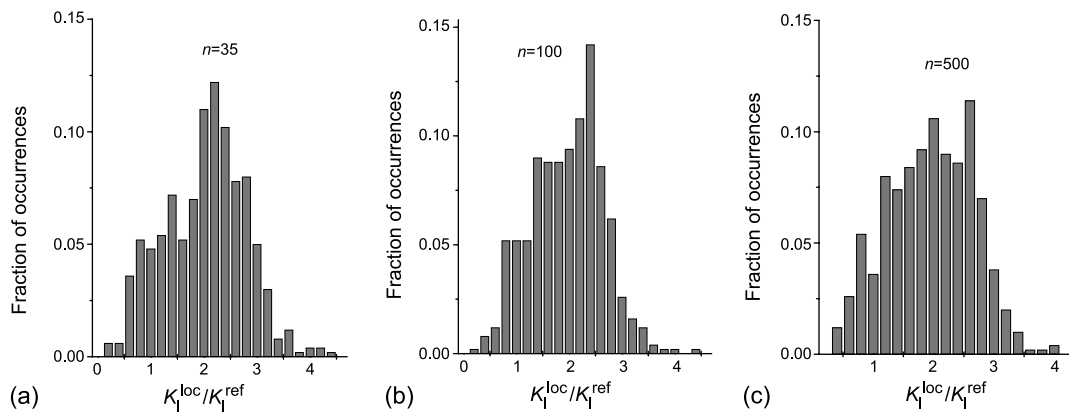
Figure 2. Histograms of normalized microscopic stress intensity factors of the cracked polycrystalline plate.

to the average moduli of the uncracked polycrystalline plate, as calculated using the same Monte Carlo procedure. The effective moduli are strong functions of the elastic constants of the grain and grain boundary. The results presented in Figure 2 correspond to $\bar{\mu}/\mu_{\mathrm{g}} = 0.14$ and $\bar{\nu} = 0.4$ (calculated for $\mu_{\mathrm{gb}}/\mu_{\mathrm{g}} = 0.004$, $\nu_{\mathrm{g}} = 0.2$, $\nu_{\mathrm{gb}} = 0.49$ and $t/d = 0.082$) and are representative of those calculated for a wide range of mismatch between the elastic moduli of the grains and the grain boundaries. They show that the statistics of the local stress intensity factors are not sensitive to the number of grains surrounding the crack tip; they depend only on the mismatch between the elastic moduli of the grain containing the crack tip and those of the surrounding effective medium.
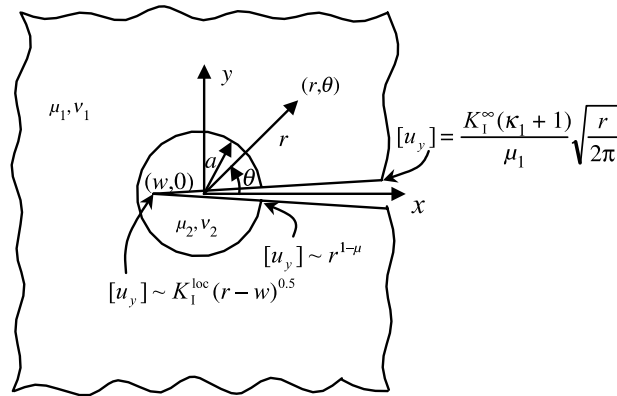
Figure 3. A semi-infinite crack penetrating a circular inhomogeneity in an infinite plane.

These results suggest that the stress intensity factors of a crack in a polycrystalline plate can be approximated by that of a long crack penetrating a circular inhomogeneity (Figure 3), as long as the elastic moduli of the inhomogeneity, μ_2, ν_2, are set equal to those of the grains (μ_g, ν_g) and the moduli of the surrounding material, μ_1, ν_1, are set equal to the effective moduli of the polycrystalline plate containing no crack ($\bar{\mu}$ and $\bar{\nu}$). This paper presents an analytic solution to the simplified micromechanical model, and confirms the validity of the approximation.

The discussion is organized as follows. Section 2 presents the stresses and displacements produced by the interaction between an inhomogeneity and edge dislocations. These Greens functions are used in Section 3 to formulate the micromechanical model as a system of singular integral equations whose solution is calculated using a numerical procedure. The results are presented and discussed in Section 4.

2. Greens Functions for Edge Dislocations Interacting with a Circular Inhomogeneity

This section presents the solutions to the plane elastostatics problems shown in Figure 4, where an infinitely extended plate contains a perfectly bonded circular inhomogeneity interacting with edge dislocations positioned inside (Figure 4(a)) and outside (Figure 4(b)) the
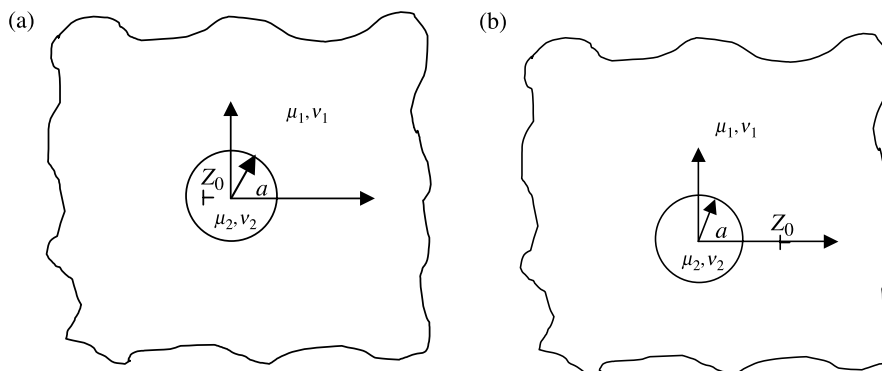
Figure 4. (a) Edge dislocation inside a circular inhomogeneity; (b) edge dislocation outside a circular inhomogeneity.

region defined by the inhomogeneity. The Airy stress functions for both cases are well known (Dundurs, 1969). For the case where the dislocation is outside the inhomogeneity, Miller and Young (1987) derived the solution in terms of complex potentials. Their procedure is used in this paper to derive the complex potentials for the case where the dislocation is inside the inhomogeneity. The reason for repeating Miller and Young's exercise is to provide the complex potentials for both cases, because the complex variable representation is more convenient for use in mixed-mode crack problems that require numerical solution of the integral equations.

These solutions are the Green's functions for the micromechanical model shown in Figure 3; they provide the displacement discontinuity across the line that defines the crack. The stresses and displacements can be conveniently represented as (Muskhelishvili, 1953)

$$\sigma_{rr} + i\tau_{r\theta} = \Phi_i(z) + \overline{\Phi_i(z)} - \frac{\bar{z}}{z}[z\overline{\Phi'_i(z)} + \overline{\Psi_i(z)}] \tag{1}$$

$$\sigma_{\theta\theta} + i\tau_{r\theta} = \Phi_i(z) + \overline{\Phi_i(z)} + \frac{z}{\bar{z}}[\bar{z}\Phi'_i(z) + \Psi_i(z)] \tag{2}$$

$$\frac{\partial}{\partial\theta}(u_x + iu_y) = \frac{iz}{2\mu_i}\left\{\kappa_i\Phi_i(z) - \overline{\Phi_i(z)} + \frac{\bar{z}}{z}[z\overline{\Phi'_i(z)} + \overline{\Psi_i(z)}]\right\} \tag{3}$$

where the potentials Φ_i, Ψ_i are analytic functions of $z = x + iy$, subscript $i = 1, 2$ denotes the regions $|z| > a$ and $|z| < a$, $\kappa_i = (3 - 4\nu_i)$ for plane strain, and $\kappa_i = (3 - \nu_i)/(1 + \nu_i)$ for plane stress.

The elastic mismatch is quantified through the constants (Dundurs, 1969)

$$\alpha = \frac{\mu_2(\kappa_1 + 1) - \mu_1(\kappa_2 + 1)}{\mu_2(\kappa_1 + 1) + \mu_1(\kappa_2 + 1)} \tag{4}$$

$$\beta = \frac{\mu_2(\kappa_1 - 1) - \mu_1(\kappa_2 - 1)}{\mu_2(\kappa_1 + 1) + \mu_1(\kappa_2 + 1)} \tag{5}$$

The continuity of stresses and displacements along the circular interface are written as

$$[\sigma_{rr} + i\tau_{r\theta}]^+ - [\sigma_{rr} + i\tau_{r\theta}]^- = 0 \tag{6}$$

$$\frac{\partial}{\partial\theta}\{[u_x + iu_y]^+ - [u_x + iu_y]^-\} = 0 \tag{7}$$

where superscript '+' ('−') indicates the limiting value as z approaches the interface from outside (inside) the inhomogeneity.

As shown in the Appendix, for the dislocation positioned at point z_0 inside the inhomogeneity, the complex potentials are

$$\Phi_1(z) = \frac{A}{z - z_0}\left(\frac{1 - \alpha}{1 + \beta}\right) + \frac{\beta - \alpha}{1 + \alpha}\frac{\bar{B}}{z} + \frac{\alpha^2 - \beta^2}{(1 + \alpha)(1 + \beta)}\frac{A}{z} \tag{8}$$

$$\Psi_1(z) = \left(\frac{1 - \alpha}{1 - \beta}\right)\left[\frac{B}{z - z_0} + \frac{A\bar{z}_0}{(z - z_0)^2}\right] + $$
$$+ \frac{a^2}{z^2}\left\{\Phi_1(z) - z\Phi'_1(z) - \frac{(1 - \alpha)}{(1 - \beta)}\left[\frac{A}{z - z_0} + \frac{zA}{(z - z_0)^2}\right] - \right.$$
$$\left. - \left[\frac{(\beta - \alpha)(\alpha + \beta)}{(1 + \alpha)(1 - \beta)}B + \frac{\alpha + \beta}{1 + \alpha}\bar{A}\right]\frac{z}{a^2} + \frac{1 - \alpha}{1 - \beta}\bar{H}\right\} \tag{9}$$

$$\Phi_2(z) = \frac{A}{z - z_0} - \left(\frac{\alpha - \beta}{1 - \beta}\right)\left\{\frac{\bar{A}}{a^2/z - \bar{z}_0} + \frac{a^2}{z}\left[\frac{\bar{A}}{(a^2/z - \bar{z}_0)^2}\right] - \right.$$
$$\left. - \frac{a^2}{z^2}\left[\frac{\bar{B}}{a^2/z - \bar{z}_0} + \frac{z_0\bar{A}}{(a^2/z - \bar{z}_0)^2}\right] + \frac{\bar{B}}{z}\right\} + \frac{(\alpha - \beta)}{(1 - \beta)}H \tag{10}$$

$$\Psi_2(z) = \frac{B}{z - z_0} + \frac{A\bar{z}_0}{(z - z_0)^2} + \frac{a^2}{z^2}\left\{\Phi_2(z) - z\Phi_2'(z) + \frac{\alpha + \beta}{1 + \beta} \times \right.$$
$$\left. \times \left(\frac{\bar{A}}{a^2/z - \bar{z}_0} - \frac{\bar{A}}{a^2}z\right) - \frac{A}{z - z_0} - \frac{zA}{(z - z_0)^2} + \bar{H}\right\} \tag{11}$$

where constants A and B are proportional to the Cartesian components, $[u_x]$ and $[u_y]$, of the displacement discontinuity

$$A = \bar{B} = \frac{\mu_2\{[u_x] + i[u_y]\}}{\pi i(\kappa_2 + 1)} \tag{12}$$

and

$$H = \frac{1}{(\alpha - 1)(1 + \alpha - 2\beta)}\frac{[-(\alpha - \beta)^2(\bar{B}\bar{z}_0 + \bar{A}z_0) + (\alpha - \beta)(1 - \beta)(Bz_0 + A\bar{z}_0)]}{a^2} \tag{13}$$

If the dislocation is outside the inhomogeneity, the potentials are

$$\Phi_1(z) = \frac{A}{z - z_0} - \frac{\beta - \alpha}{1 + \beta}\left\{\frac{\bar{A}}{a^2/z - \bar{z}_0} + \frac{a^2}{z}\left[\frac{\bar{A}}{(a^2/z - \bar{z}_0)^2}\right] - \right.$$
$$\left. - \frac{a^2}{z^2}\left[\frac{\bar{B}}{a^2/z - \bar{z}_0} + \frac{z_0\bar{A}}{(a^2/z - \bar{z}_0)^2}\right] + \frac{\bar{A}}{\bar{z}_0}\right\} \tag{14}$$

$$\Psi_1(z) = \frac{B}{z - z_0} + \frac{A\bar{z}_0}{(z - z_0)^2} + \frac{a^2}{z^2}\left\{\Phi_1(z) - z\Phi_1'(z) + \left(\frac{\alpha + \beta}{\beta - 1}\right)\frac{\bar{A}}{a^2/z - \bar{z}_0} - \right.$$
$$\left. - \frac{A}{z - z_0} - \frac{zA}{(z - z_0)^2} - \frac{A}{z_0} + \left(\frac{1 - \alpha}{1 - \beta}\right)\bar{C}\right\} \tag{15}$$

$$\Phi_2(z) = \left(\frac{1 + \alpha}{1 - \beta}\right)\frac{A}{z - z_0} + \left(\frac{\alpha - \beta}{1 - \beta}\right)C \tag{16}$$

$$\Psi_2(z) = \left(\frac{1 + \alpha}{1 + \beta}\right)\left[\frac{B}{z - z_0} + \frac{A\bar{z}_0}{(z - z_0)^2}\right] + $$
$$+ \frac{a^2}{z^2}\left\{\Phi_2(z) - z\Phi_2'(z) - \left(\frac{1 + \alpha}{1 + \beta}\right)\left[\frac{A}{z - z_0} + \frac{zA}{(z - z_0)^2} + \frac{A}{z_0}\right] + \bar{C}\right\} \tag{17}$$

where

$$C = \frac{(1 + \alpha)}{(\alpha - 1)(1 + \alpha - 2\beta)}\left[(\alpha - \beta)\frac{A}{z_0} - (1 - \beta)\frac{\bar{A}}{\bar{z}_0}\right], \qquad A = \bar{B} = \frac{\mu_1\{[u_x] + i[u_y]\}}{\pi i(\kappa_1 + 1)} \tag{18}$$

3. Singular Integral Equations

The zero traction boundary condition along the crack surfaces shown in Figure 3 is written as

$$\sigma_{\theta\theta} + i\tau_{r\theta} = 0 \qquad w < x < \infty \tag{19}$$

The stress combination in equation (19) produced at any point z by discrete dislocations inside and outside the circular inhomogeneity is readily evaluated through equations (2), (8)–(11) and (14)–(17). For the mode-I case considered here, $[u_x] = 0$, and the stresses can be written symbolically as

$$\sigma_{\theta\theta} + i\tau_{r\theta} = \frac{2B_1}{x-t} + B_1 K_{11}(x,t) + B_2 K_{12}(x,t) \quad a < x < \infty \tag{20}$$

$$\sigma_{\theta\theta} + i\tau_{r\theta} = \frac{2B_2}{x-t} + B_2 K_{21}(x,t) + B_1 K_{22}(x,t) \quad w < x < a \tag{21}$$

where B_1 and B_2 are proportional to the magnitude of the displacement discontinuity associated with the dislocations outside and inside the inhomogeneity, respectively. Obviously they do not satisfy the traction boundary condition. However, by introducing the dislocation densities $b_i(t) = (\mu_i / \pi i (\kappa_i + 1))(\partial\{[u_x] + i[u_y]\}/\partial t)$, the traction boundary condition along the crack surfaces can be written in the form of the coupled singular integral equations

$$\int_a^\infty \frac{2b_1(t)}{x-t}\,\mathrm{d}t + \int_a^\infty K_{11}(x,t)b_1(t)\,\mathrm{d}t + \int_w^a K_{12}(x,t)b_2(t)\,\mathrm{d}t = 0 \quad x > a$$

$$\int_w^a \frac{2b_2(t)}{x-t}\,\mathrm{d}t + \int_w^a K_{21}(x,t)b_2(t)\,\mathrm{d}t + \int_a^\infty K_{22}(x,t)b_1(t)\,\mathrm{d}t = 0 \quad w < x < a \tag{22}$$

The first integral in each of equations (22) contains a Cauchy kernel. The K_{ij} are combinations of regular and generalized kernels, the latter being unbounded when $x = a$ and $t = a$. The asymptotic form of the dislocation densities at the endpoints of the integration intervals, and the relationships between them at the interface, can be derived using the function theoretic method (Muskhelishvili, 1953) or the Williams technique (1957). The following results are obtained: (i) b_2 (or alternatively the stress) at a distance r from the origin has the well known asymptotic form $K_1^{\mathrm{loc}}(r-w)^{-1/2}$, where K_1^{loc} is the microscopic stress intensity factor; (ii) b_1 and b_2 are of the form $r^{-\mu}$ at the interface between the inhomogeneity and the surrounding material, where (Erdogan and Gupta, 1975) μ is the root of

$$(1-\beta^2)(1+\cos^2\mu\pi) + 2[2\alpha\beta - 1 - (2\alpha\beta - \beta^2)\cos\mu\pi] + 4\mu(2-\mu)$$
$$[(\alpha-\beta)^2(1-\mu)^2 - \alpha\beta + \beta(\alpha-\beta)\cos\mu\pi] = 0 \tag{23}$$

(iii) the dislocation densities satisfy the following condition at the interface (Erdogan and Gupta, 1975; Erdogan *et al.*, 1973)

$$\lim_{t\to a^+} \frac{b_2(-t)}{b_1(t)} = F(\alpha, \beta, \mu)\left(\frac{\mu_2(\kappa_1 + 1)}{\mu_1(\kappa_2 + 1)}\right) \tag{24}$$

where

$$F(\alpha, \beta, \mu) = \frac{(1+\alpha)\beta + (\alpha-\beta)(1-\beta)(-1+4\mu-2\mu^2) - (1-\beta^2)\cos(\mu\pi)}{(1+\alpha)(-1+2\beta-2\beta\mu)} \tag{25}$$

The loci of μ in the $\alpha - \beta$ are shown in Figure 5(a).
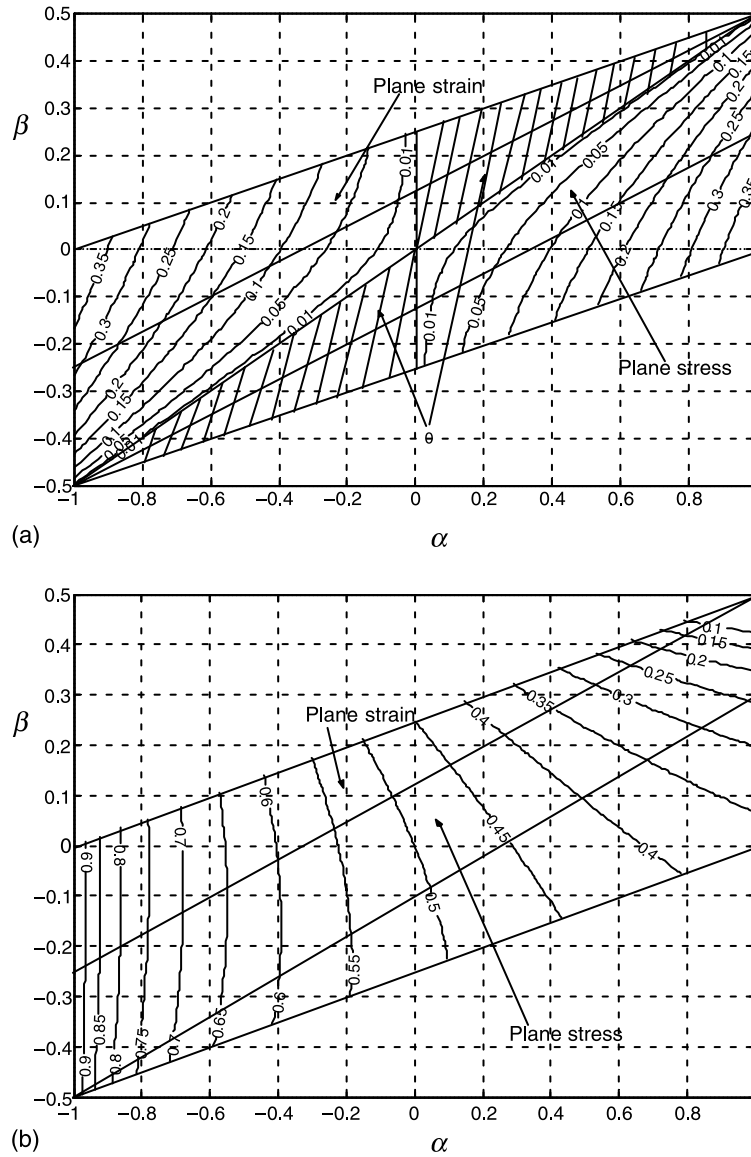
Figure 5. (a) The loci of parameter μ in the α–β plane; (b) the loci of parameter λ in the α–β plane.

Equations (22) are homogeneous; they do not have a unique solution because the loading is not yet prescribed. A unique solution can be obtained by introducing a far-field loading that corresponds to a nominal stress intensity factor K_I^∞, which is equivalent to the condition that $b_1(t) \rightarrow \frac{K_I^\infty}{2\pi\sqrt{2\pi}\sqrt{t}}$ as $t \rightarrow \infty$. To this end, the dislocation density functions are expressed in terms of the regular functions $g_1(t)$, $g_2(t)$ and $g^\infty(t)$ as

$$b_1(t) = \frac{K_I^\infty}{(t-w)^{0.5-\mu}(t-a)^\mu}[g_1(t) + g^\infty(t)] \qquad (26)$$

$$b_2(t) = \frac{K_I^\infty}{(t-w)^{0.5}(a-t)^\mu}g_2(t) \qquad (27)$$

These representations, together with the condition $g_1(t) \to 0$, as $t \to \infty$, provide the correct asymptotic behavior and prescribed loading. Different functions of $g^\infty(t)$ can be adopted, which may affect the convergence rate of the numerical solution described below. The form taken in this study is

$$g^\infty(t) = \frac{(1 - e^{-(t-a)^2})}{2\pi\sqrt{2\pi}} \tag{28}$$

Substitution of equations (26)–(28) into (22) results in a nonhomogeneous system of integral equations. Nondimensional forms of the dislocation densities, $\bar{b}_i$, regular functions, $\bar{g}_i$, and length parameters, η and ξ, are introduced to convert the integration intervals to interval $[-1,1]$. The resulting equations are solved numerically using the approach developed by Erdogan *et al.* (1973), which relies on the properties of Gauss–Jacobi polynomials to approximate the nondimensional dislocation densities (which are of the form $\bar{b}_i(\eta) = (1-\eta)^{s_1}$ $(1+\eta)^{s_2}\bar{g}_i(\eta)$, $-1 < \mathrm{Re}[s_i] < 0$) and in turn the nondimensionalized forms of the integrals that appear in equation (22) as

$$\int_{-1}^{1} \frac{\bar{b}_i(\eta)}{\xi - \eta}\mathrm{d}\eta \approx \sum_{k=1}^{N} W_k \frac{\bar{g}_i(\eta_k)}{\xi_j - \eta_k} \tag{29}$$

$$\int_{-1}^{1} K_{mn}(\eta, \xi)\bar{b}_i(\eta)\mathrm{d}\eta \approx \sum_{k=1}^{N} W_k K_{mn}(\xi_j, \eta_k)\bar{g}_i(\eta_k) \quad i, m, n = 1, 2 \tag{30}$$

The N integration points η_k are the roots of Jocobi polynomial $P_N^{(s_1,s_2)}(\eta_k) = 0, k = 1, \ldots N$, the collocation points ξ_j are the roots of Jocobi polynomi $P_{N-1}^{(s_1+1,s_2+1)}(\xi_j) = 0$, $j = 1, \ldots N - 1$, and the weights are given by

$$W_k = -\frac{2N + s_1 + s_2 + 2}{(N + 1)!(N + s_1 + s_2 + 1)} \times$$
$$\times \frac{\Gamma(N + s_1 + 1)\Gamma(N + s_2 + 1)}{\Gamma(N + s_1 + s_2 + 1)} \frac{2^{s_1+s_2}}{P_N'^{(s_1,s_2)}(\eta_k) P_{N+1}^{(s_1,s_2)}(\eta_k)} \tag{31}$$

Thus the integral equations are reduced to a system of $2(N-1)$ linear algebraic equations with $2N$ unknowns. The additional two equations required for solution are the previously stated far field condition $g_1(t) \to 0$, as $t \to \infty$ and the interface compatibility condition given by equation (24).

The normalized microscopic stress intensity factor is related to the regular part of the dislocation density at the crack-tip, through the formula

$$\frac{K_I^{\mathrm{loc}}}{K_I^\infty} = \frac{2\pi\sqrt{2\pi}}{(a - w)^\mu}g_2(w) \tag{32}$$

4. Results and Discussion

The variation with elastic mismatch of the normalized microscopic stress intensity factor corresponding to the crack-tip at the center of the inhomogeneity is shown in Figure 6. The
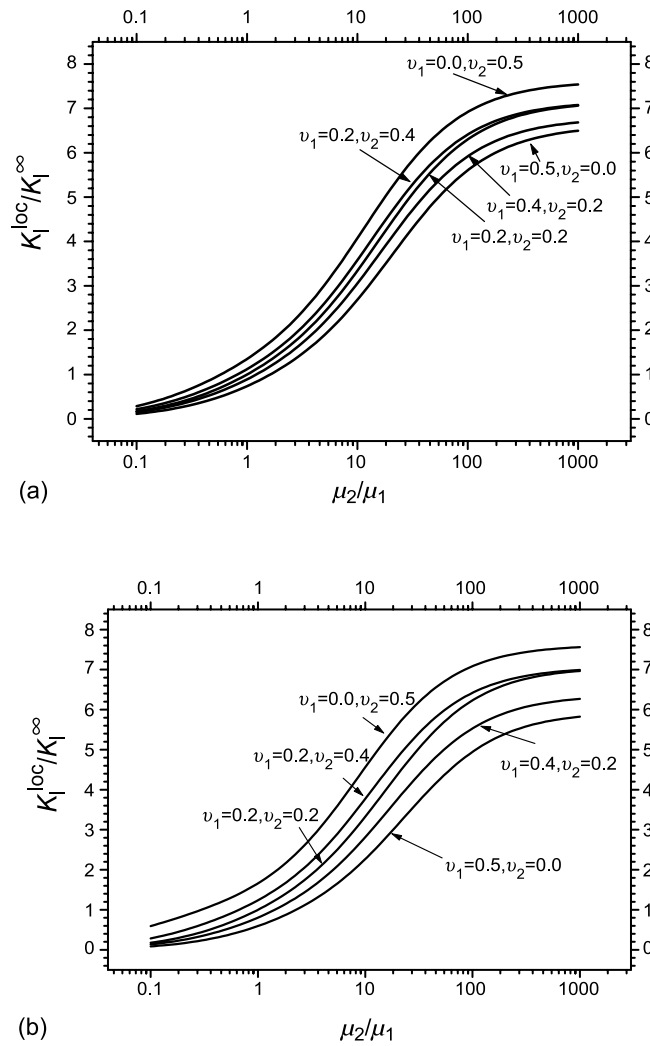
Figure 6. Normalized microscopic stress intensity factor as functions of ratio of shear moduli for (a) plane strain, and (b) plane stress.

plane strain results agree to within 2% with those obtained by Steif (1987) using a conformal mapping technique (Steif noted that his procedure is slowly converging in regions of the parameter space).

The stress intensity factor variation as the crack traverses the inhomogeneity from right to left is shown in Figure 7 for selected values of elastic mismatch. Figure 7(a) shows that if the inhomogeneity is stiffer than the surrounding material, then the stress intensity factor starts out as zero, and as it approaches the other side it increases without bound. Figure 7(b) shows the opposite trend when the inhomogeneity is more compliant than the surrounding material.

Figure 8 illustrates that when the crack-tip is at distances from the interface ε that are much smaller than the radius of the inhomogeneity, the numerical procedure breaks down. To calculate the stress intensity factors associated with this small parameter, the formulation introduced by Romeo and Ballarini (1995) is used. They showed that the microscopic stress
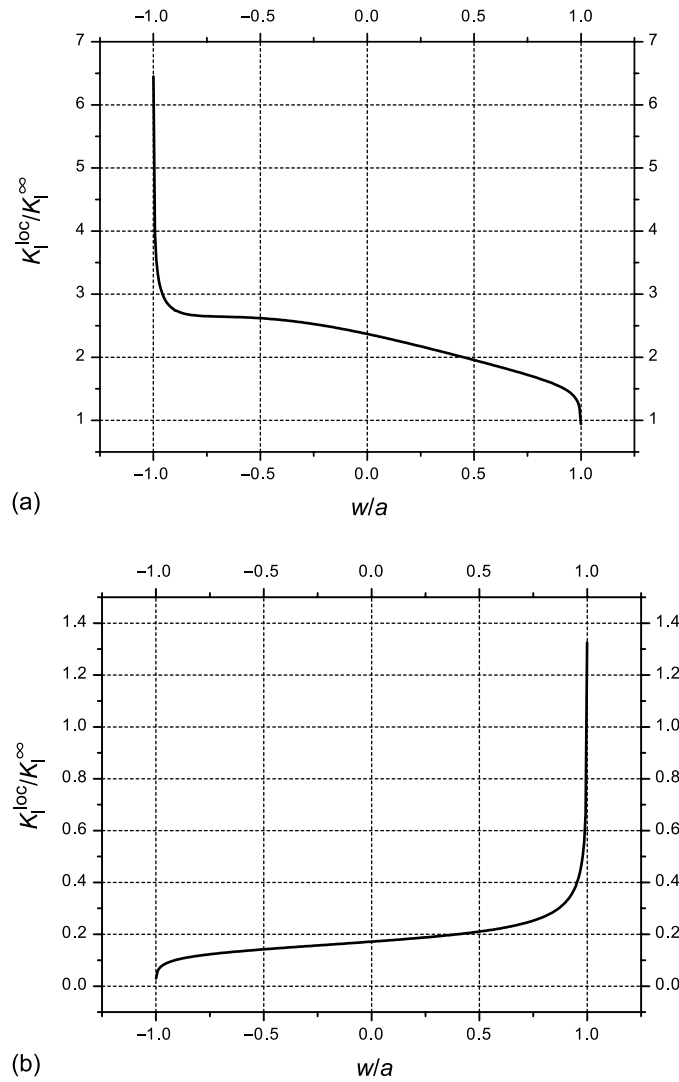
Figure 7. Variation of normalized microscopic stress intensity factor as the crack traverses the inhomogeneity for the parameters (a) $\mu_1/\mu_2 = 0.14$, $\kappa_1 = 1.40$, $\kappa_2 = 2.2$ ($\alpha = 0.6812$, $\beta = 0.0735$) and (b) $\mu_1/\mu_2 = 10$, $\kappa_1 = \kappa_2 = 2.6$ ($\alpha = -0.8182$, $\beta = -0.3636$).

intensity factor can be written in the form

$$\frac{K_{\mathrm{I}}^{\mathrm{loc}}}{K_{\mathrm{I}}^{\infty}} = C\varepsilon^{(0.5-\lambda)} \tag{33}$$

where C is a type of stress intensity factor that depends on the elastic mismatch, the type of loading, and the geometry of the cracked plate, and λ is the root of

$$\cos(\lambda\pi) = \frac{3(\beta' - \alpha')}{2(1 + \beta')}(1 - \lambda)^2 + \frac{\alpha' + \beta'^2}{1 - \beta'^2} \tag{34}$$

In equation (34) $\alpha' = \alpha$ and $\beta' = \beta$ for the case where the crack has just penetrated the inhomogeneity, and $\alpha' = -\alpha$ and $\beta' = -\beta$ for the case where the crack is approaching the opposite interface. The loci of constant λ in the $\alpha - \beta$ plane are shown in Figure 5(b).
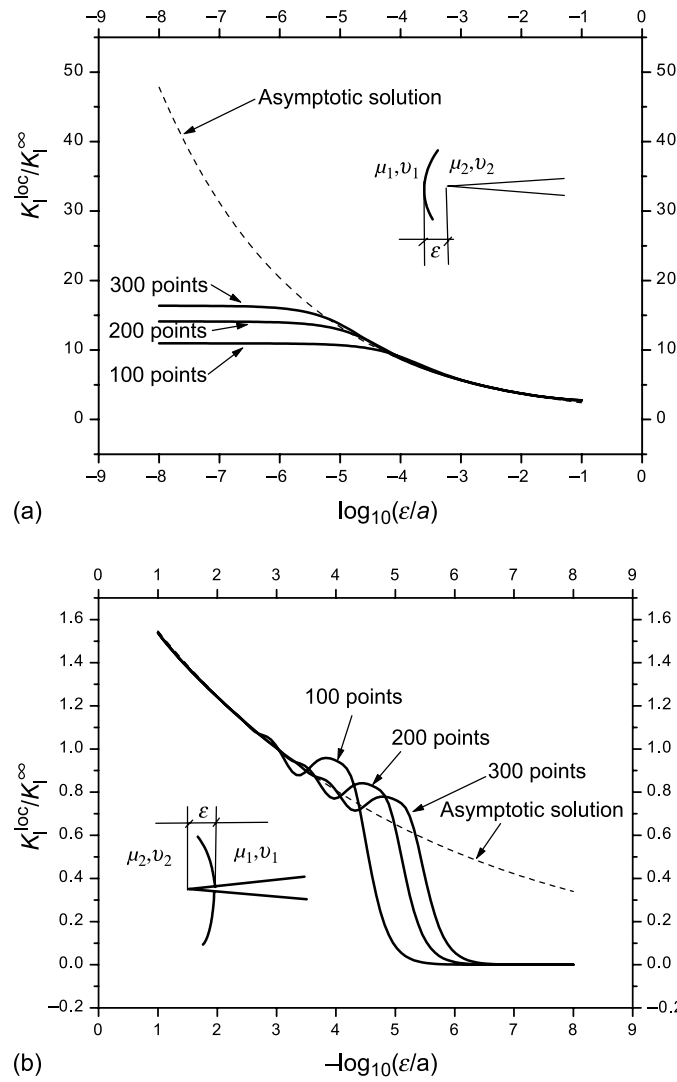
Figure 8. Variation of normalized microscopic stress intensity factor associated with $\mu_1/\mu_2 = 0.14$, $\kappa_1 = 1.40$, $\kappa_2 = 2.2$ ($\alpha = 0.6812$, $\beta = 0.0735$) and the crack tip being very close to (a) the left interface and (b) the right interface. Note that if the crack tip is close to the left interface, $\varepsilon/a = (w + a)/a$, while if it is close to the right interface, $\varepsilon/a = (a - w)/a$.

In principle the constant C could be calculated by solving an auxiliary boundary value problem, as described by Romeo and Ballarini. Here we cheat by matching equation (33) with the stress intensity factor evaluated at the smallest distance d for which the numerical procedure produces a convergent result. The resulting asymptotic solution given by equation (33) is shown as dashed lines in Figure 8.

Next we assess how well the micromechanical model predicts the stress intensity factors of the previously discussed cracked polycrystalline plate with compliant grain boundaries. For a given level of elastic mismatch, the expected value of the microscopic stress intensity factor is

$$\overline{K_{\mathrm{I}}^{\mathrm{loc}}} = \frac{d_1(1.5 - \lambda_1)K_{\mathrm{I}}^{\mathrm{loc}}(d_1) + [2a - (d_1 + d_2)](\overline{K_{\mathrm{I}}^{\mathrm{loc}}})_{\mathrm{mid}} + d_2(1.5 - \lambda_2)K_{\mathrm{I}}^{\mathrm{loc}}(d_2)}{2a} \quad (35)$$

where the first and third terms in the numerator represent the contributions to the average value of the stress intensity factor within the matching distances d_1 and d_2 (the right-most and left-most points, respectively) calculated as

$$\frac{1}{d_i} \int_0^{d_i} C\delta^{0.5-\lambda} d\delta = (1.5 - \lambda) C d_i^{0.5-\lambda} = (1.5 - \lambda) K_{\mathrm{I}}^{\mathrm{loc}}(d_i) \tag{36}$$

The average value of the normalized stress intensity factor associated with the Monte Carlo results presented in Figure 2 is equal to 2.0. The micromechanical model predicts 2.2. Moreover, it is noted that the value predicted by the micromechanical model for a crack-tip at the center of the inhomogeneity is 2.2. These results for a relatively large elastic mismatch demonstrate that the micromechanical model is a very good approximation to the cracked polycrystalline plate problem.

Appendix

Adopting the notation $\bar{f}(z) = \overline{f(\bar{z})}$, the terms in equations (3) and (4) can be written as

$$[\sigma_{rr} + i\tau_{r\theta}]^+ = [\Phi_1(z)]^+ + \left[\bar{\Phi}_1\left(\frac{a^2}{z}\right) - \frac{a^2}{z}\bar{\Phi}_1'\left(\frac{a^2}{z}\right) - \frac{a^2}{z^2}\bar{\Psi}_1\left(\frac{a^2}{z}\right) \right]^-$$

$$[\sigma_{rr} + i\tau_{r\theta}]^- = [\Phi_2(z)]^- + \left[\bar{\Phi}_2\left(\frac{a^2}{z}\right) - \frac{a^2}{z}\bar{\Phi}_2'\left(\frac{a^2}{z}\right) - \frac{a^2}{z^2}\bar{\Psi}_2\left(\frac{a^2}{z}\right) \right]^+ \tag{A.1}$$

and

$$\frac{\partial}{\partial \theta}[u_x + iu_y]^+ = aie^{i\theta}\left\{ \frac{\kappa_1}{2\mu_1}[\Phi_1(z)]^+ + \right.$$

$$\left. + \frac{1}{2\mu_1}\left[-\bar{\Phi}_1\left(\frac{a^2}{z}\right) + \frac{a^2}{z}\bar{\Phi}_1'\left(\frac{a^2}{z}\right) + \frac{a^2}{z^2}\bar{\Psi}_1\left(\frac{a^2}{z}\right) \right]^- \right\}$$

$$\frac{\partial}{\partial \theta}[u_x + iu_y]^- = aie^{i\theta}\left\{ \frac{\kappa_2}{2\mu_2}[\Phi_2(z)]^- + \right.$$

$$\left. + \frac{1}{2\mu_2}\left[-\bar{\Phi}_2\left(\frac{a^2}{z}\right) + \frac{a^2}{z}\bar{\Phi}_2'\left(\frac{a^2}{z}\right) + \frac{a^2}{z^2}\bar{\Psi}_2\left(\frac{a^2}{z}\right) \right]^+ \right\} \tag{A.2}$$

The jump conditions across the interface can be written in compact form through the introduction of jump potentials Ω_σ and Ω_u, defined as (Miller and Young, 1987)

$$\Omega_\sigma(z) = \begin{cases} \Phi_1(z) - \bar{\Phi}_2\left(\frac{a^2}{z}\right) + \frac{a^2}{z}\bar{\Phi}_2'\left(\frac{a^2}{z}\right) + \frac{a^2}{z^2}\bar{\Psi}_2\left(\frac{a^2}{z}\right), & |z| > a \\[4mm] \Phi_2(z) - \bar{\Phi}_1\left(\frac{a^2}{z}\right) + \frac{a^2}{z}\bar{\Phi}_1'\left(\frac{a^2}{z}\right) + \frac{a^2}{z^2}\bar{\Psi}_1\left(\frac{a^2}{z}\right), & |z| < a \end{cases} \tag{A.3}$$

$$\Omega_u(z) = \begin{cases} \dfrac{\kappa_1}{2\mu_1}\Phi_1(z) + \dfrac{1}{2\mu_2}\left[\bar{\Phi}_2\left(\dfrac{a^2}{z}\right) - \dfrac{a^2}{z}\bar{\Phi}_2'\left(\dfrac{a^2}{z}\right) - \dfrac{a^2}{z^2}\bar{\Psi}_2\left(\dfrac{a^2}{z}\right)\right], & |z| > a \\[4mm] \dfrac{\kappa_2}{2\mu_2}\Phi_2(z) + \dfrac{1}{2\mu_1}\left[\bar{\Phi}_1\left(\dfrac{a^2}{z}\right) - \dfrac{a^2}{z}\bar{\Phi}_1'\left(\dfrac{a^2}{z}\right) - \dfrac{a^2}{z^2}\bar{\Psi}_1\left(\dfrac{a^2}{z}\right)\right], & |z| < a \end{cases} \tag{A.4}$$

These allow the continuity conditions to be expressed as Hilbert problems

$$[\sigma_{rr} + i\tau_{r\theta}]^+ - [\sigma_{rr} + i\tau_{r\theta}]^- = \Omega_\sigma^+ - \Omega_\sigma^- = 0 \tag{A.5}$$

$$\frac{\partial}{\partial\theta}\{[u_x + iu_y]^+ - [u_x + iu_y]^-\} = aie^{i\theta}\{\Omega_u^+ - \Omega_u^-\} = 0 \tag{A.6}$$

First consider a dislocation at point z_0 inside the inhomogeneity. The potentials for the regions inside and outside the inhomogeneity are written as

$$\begin{aligned} \Omega_\sigma &= \Omega_\sigma^0 + \Omega_\sigma^c + P_\sigma^m(z) + R_\sigma^m(z) \\ \Omega_u &= \Omega_u^0 + \Omega_u^c + P_u^m(z) + R_u^m(z) \end{aligned} \tag{A.7}$$

where Ω_σ^0 and Ω_u^0 represent the free space potentials (Greens functions) for a dislocation at z_0, 'correction terms' Ω_σ^c and Ω_u^c are required to satisfy equations (A.5) and (A.6), and the

$$\begin{aligned} R_\sigma^m(z) &= \frac{c_{\sigma 1}}{(z - z_k)} + \frac{c_{\sigma 2}}{(z - z_k)^2} + \cdots + \frac{c_{\sigma m}}{(z - z_k)^m}, \\ R_u^m(z) &= \frac{c_{u1}}{(z - z_k)} + \frac{c_{u2}}{(z - z_k)^2} + \cdots + \frac{c_{um}}{(z - z_k)^m}, \\ P_\sigma^m(z) &= P_{\sigma 0} + P_{\sigma 1}z + P_{\sigma 2}z^2 + \cdots + P_{\sigma m}z^m, \\ P_u^m(z) &= P_{u0} + P_{u1}z + P_{u2}z^2 + \cdots + P_{um}z^m \end{aligned}$$

are available to eliminate unwanted singularities introduced by the correction terms.

The free space Green's functions are given by

$$\Phi_1^0(z) = \Psi_1^0(z) = 0, \qquad \Phi_2^0(z) = \frac{A}{z - z_0}, \qquad \Psi_2^0(z) = \frac{B}{z - z_0} + \frac{A\bar{z}_0}{(z - z_0)^2} \tag{A.8}$$

where the constants A and B are related to the Burgers vector, written in terms of the components of displacement discontinuities $[u_x]$ and $[u_y]$

$$A = \bar{B} = \frac{\mu_2\{[u_x] + i[u_y]\}}{\pi i(\kappa_2 + 1)} \tag{A.9}$$

Conversion of these potentials through into the associated jump potential leads to.

$$\Omega_\sigma^0(z) = \begin{cases} -\dfrac{\bar{A}}{a^2/z - \bar{z}_0} - \dfrac{a^2}{z}\left[\dfrac{\bar{A}}{(a^2/z - \bar{z}_0)^2}\right] + \dfrac{a^2}{z^2}\left[\dfrac{\bar{B}}{a^2/z - \bar{z}_0} + \dfrac{z_0\bar{A}}{(a^2/z - \bar{z}_0)^2}\right], & |z| > a \\[4mm] \dfrac{A}{z - z_0}, & |z| < a \end{cases} \tag{A.10}$$

$$\Omega_u^0(z) = \begin{cases} \dfrac{1}{2\mu_2}\left\{\dfrac{\bar{A}}{a^2/z - \bar{z}_0} + \dfrac{a^2}{z}\left[\dfrac{\bar{A}}{(a^2/z - \bar{z}_0)^2}\right] - \dfrac{a^2}{z^2}\left[\dfrac{\bar{B}}{a^2/z - \bar{z}_0} + \dfrac{z_0\bar{A}}{(a^2/z - \bar{z}_0)^2}\right]\right\}, & |z| > a \\[4mm] \dfrac{\kappa_2}{2\mu_2}\dfrac{A}{z - z_0}, & |z| < a \end{cases} \tag{A.11}$$

These obviously do not satisfy the continuity conditions across the interface. The correction terms are readily identified by Equations (A.12) and (A.13) as

$$\Omega_\sigma^c(z) = \begin{cases} \dfrac{A}{z-z_0}, & |z| > a \\[2mm] -\dfrac{\bar{A}}{a^2/z-\bar{z}_0} - \dfrac{a^2}{z}\left[\dfrac{\bar{A}}{(a^2/z-\bar{z}_0)^2}\right] + \dfrac{a^2}{z^2}\left[\dfrac{\bar{B}}{a^2/z-\bar{z}_0} + \dfrac{z_0\bar{A}}{(a^2/z-\bar{z}_0)^2}\right], & |z| < a \end{cases} \qquad (A.12)$$

$$\Omega_u^c(z) = \begin{cases} \dfrac{\kappa_2}{2\mu_2}\dfrac{A}{z-z_0}, & |z| > a \\[2mm] \dfrac{1}{2\mu_2}\left\{\dfrac{\bar{A}}{a^2/z-\bar{z}_0} + \dfrac{a^2}{z}\left[\dfrac{\bar{A}}{(a^2/z-\bar{z}_0)^2}\right] - \dfrac{a^2}{z^2}\left[\dfrac{\bar{B}}{a^2/z-\bar{z}_0} + \dfrac{z_0\bar{A}}{(a^2/z-\bar{z}_0)^2}\right]\right\}, & |z| < a \end{cases} \qquad (A.13)$$

The combinations $\Omega_\sigma^0 + \Omega_\sigma^c$ and $\Omega_u^0 + \Omega_u^c$ introduce unwanted singularities at the origin, which are eliminated by taking

$$R_\sigma + P_\sigma = H + \frac{M}{z} \qquad (A.14)$$

and

$$R_u + P_u = P + \frac{N}{z} \qquad (A.15)$$

After some algebra that involves the Taylor expansion

$$\frac{\bar{A}}{a^2/z - z_0} = \frac{\bar{A}z}{a^2}\left[1 + \frac{zz_0}{a^2} + \frac{1}{2}\frac{(zz_0)^2}{a^4} + O(z^3)\right], \quad \text{as } z \to 0 \qquad (A.15a)$$

the constants are obtained as

$$M = \frac{\beta - \alpha}{1 + \alpha}\bar{B} - \frac{\alpha + \beta}{1 + \alpha}A \qquad (A.16)$$

$$N = \frac{\kappa_1}{2\mu_1}\frac{\beta - \alpha}{1 + \alpha}\bar{B} + \frac{1}{2\mu_1}\frac{\alpha + \beta}{1 + \alpha}A \qquad (A.17)$$

$$P = -\frac{1}{2\mu_2}H \qquad (A.18)$$

$$H = \frac{1}{(\alpha - 1)(1 + \alpha - 2\beta)}[-(\alpha - \beta)^2(\bar{B}\bar{z}_0 + \bar{A}z_0) + \\ + (\alpha - \beta)(1 - \beta)(Bz_0 + A\bar{z}_0)]/a^2 \qquad (A.19)$$

For the dislocation outside the inhomogeneity, the procedure is repeated by starting with $\Phi_2^0(z) = \Psi_2^0(z) = 0$, $\Phi_1^0(z) = A/(z - z_0)$ and $\Psi_1^0(z) = B/(z - z_0) + A\bar{z}_0/(z - z_0)^2$. For this

case it suffices to introduce $R_\sigma + P_\sigma = L$ and, $R_u + P_u = K$, where

$$L = -\frac{\bar{A}}{\bar{z}_0} + C \tag{A.20}$$

$$K = \frac{1}{2\mu_1}\frac{\bar{A}}{\bar{z}_0} - \frac{C}{2\mu_2} \tag{A.21}$$

$$C = \frac{(1+\alpha)}{(\alpha-1)(1+\alpha-2\beta)}\left[(\alpha-\beta)\frac{A}{z_0} - (1-\beta)\frac{\bar{A}}{\bar{z}_0}\right] \tag{A.22}$$

References

1. Abdel-Tawab, K. and Rodin, G., 'On the relevance of linear elastic fracture mechanics to ice', *Int. J. Fracture* **62** (1993) 171-181.
2. Ballarini, R., Mullen, R.L. and Heuer, A.H., 'The effects of heterogeneity and anisotropy on the size effect in cracked polycrystalline films', *Int. J. Fracture* **95** (1999) 19–39.
3. Dundurs, J., 'Elastic interaction of dislocations with inhomogeneities', in: T. Mura (ed.), *Mathematical Theory of Dislocations*, ASME, 1969, pp. 368–425.
4. Erdogan, F. and Biricikoglu, V., 'Two bonded half planes with a crack going through the interface', *Int. J. Eng. Sci.* **11** (1973) 745–766.
5. Erdogan, F. and Gupta, G.D., 'The inclusion problem with a crack crossing the boundary', *Int. J. Fracture* **11**(1) (1975) 13–27.
6. Erdogan, F., Gupta, G.D. and Cook, T.S., 'Numerical solution of singular integral equations', in: G.C. Sih (ed.), *Mechanics of Fracture*, Vol. 1, Chapter 7, Noordhoff, 1973, pp. 368–425.
7. Miller, G.R. and Young, R.P., 'On singular solutions for inclusion problems in plane elasticity', *J. Appl. Mech. ASME* **54** (1987) 738–740 (Brief Note).
8. Muskhelishvili, N.I., *Some Basic Problems of the Mathematical Theory of Elasticity*, Noordhoff, Holland, 1953a.
9. Muskhelishvili, N.I., *Singular Integral Equations*, Noordhoff, Holland, 1953b.
10. Romeo, A. and Ballarini, R., 'A crack very close to a bimaterial interface', *J. Appl. Mech.* **62** (1995) 614–619.
11. Steif, P.S., 'A semi-infinite crack partially penetrating a circular inclusion', *J. Appl. Mech.* **54** (1987) 87–92.
12. Wang, Y. and Ballarini, R., 'The effects of grain boundary stiffness on the stress intensity factors of a crack in a polycrystalline film' (submitted for publication) (2002).
13. Williams, M.L., 'On the stress distribution at the base of a stationary crack', *J. Appl. Mech.* **24** (1957) 109–114.